Eur Biophys J (2004) 33: 549–554
DOI 10.1007/s00249-004-0396-1

ARTICLE

**Neslihan Toyran · Faruk Zorlu · Gizem Dönmez
Kamil Öğe · Feride Severcan**

Chronic hypoperfusion alters the content and structure of proteins and lipids of rat brain homogenates: a Fourier transform infrared spectroscopy study

Received: 18 September 2003 / Revised: 20 January 2004 / Accepted: 5 February 2004 / Published online: 16 March 2004

Abstract Arteriovenous malformations (AVMs), masses of abnormal blood vessels which grow in the brain, produce high flow shunts that steal blood from surrounding brain tissue, which is chronically hypoperfused. Hypoperfusion is a condition of inadequate tissue perfusion and oxygenation, resulting in abnormal tissue metabolism. Fourier transform infrared (FTIR) spectroscopy is used in this study to investigate the effect of hypoperfusion on homogenized rat brain samples at the molecular level. The results suggest that the lipid content increases, the protein content decreases, the lipid-to-protein ratio increases, and the state of order of the lipids increases in the hypoperfused brain samples. FTIR results also revealed that, owing to hypoperfusion, not only the protein synthesis but also the protein secondary structure profile is altered in favor of β-sheets and random coils. These findings clearly demonstrate that, FTIR spectroscopy can be used to extract valuable information at the molecular level so as to have a better understanding of the effect of hypoperfusion on rat brain.

Keywords Brain · Hypoperfusion · Macromolecules · Secondary structure · Fourier transform infrared spectroscopy

N. Toyran · G. Dönmez · F. Severcan (✉)
Department of Biology, Middle East Technical University, 06531 Ankara, Turkey
E-mail: feride@metu.edu.tr
Tel.: +90-312-2105166
Fax: +90-312-2101289

F. Zorlu
Department of Radiation Oncology, Faculty of Medicine, Hacettepe University, 06100 Sıhhıye, Ankara, Turkey

K. Öğe
Department of Neurosurgery, Faculty of Medicine, Hacettepe University, 06100 Sıhhıye, Ankara, Turkey

Introduction

Arteriovenous malformations (AVMs) are congenital vascular malformations that bypass the blood from the arterial side to the venous side, mimicking an arteriovenous fistula. Because of this bypass, blood in the arterial side drains to the venous side and this drainage causes a hypoperfusion on the surrounding brain tissue, which is called as the steal phenomenon. This phenomenon is caused by the diversion of the blood flow from high-resistance tissue capillaries to low-resistance AVM nidus. The steal phenomenon usually presents itself clinically with hypoxic symptoms. AVM can occur in any area of the brain, and may be either small or large.

AVMs come to clinical attention mainly in young adults, typically before the age of 40. It was reported in a previous study that about 53% of patients with AVMs present with a hemorrhage (Hofmeister et al. 2000). In addition to this, chronic cerebral hypoperfusion is also shown to cause learning and memory impairments (Wang et al. 2000).

In the case of hypoperfusion, there is a reduction of both oxygen and glucose supplies (Kawaguchi et al. 2002). Since brain cells are unusually sensitive to oxygen lack (Siesjo 1988) and glucose is the only substrate used by the brain, it is very crucial to investigate the effect of hypoperfusion on the brain. The effect of hypoxia (Kral et al. 1993; Fleidervish et al. 2001; Yamada et al. 2001) and the influence of glucose deprivation (Alici and Heinemann 1995; Alici et al. 1998) on different regions of the brain have been investigated previously by many scientists. Despite some studies on the effect of hypoperfusion on the brain (Shi et al. 2000; Takagi et al. 2000; Wang et al. 2000; de Wilde et al. 2002; Kawaguchi et al. 2002; Roman et al. 2002), the precise mechanism of hypoperfusion-induced changes on brain tissue still remains to be elucidated at the molecular level. The aim of this study is to obtain a more detailed picture about this effect at the molecular level by using Fourier transform infrared (FTIR) spectroscopy. It is a non-disturbing

technique which provides quantitative biochemical information about biological samples (Choo et al. 1993; Sills et al. 1994; Liu et al. 1996; Jackson et al. 1997; Wetzel et al. 1998; Diem et al. 1999; Liu et al. 2002; Çakmak et al. 2003; Mourant et al. 2003). It is a valuable technique due to its high sensitivity in detecting changes in the functional groups belonging to tissue components, such as lipids, proteins and nucleic acids (Fabian et al. 1995; Kneipp et al. 2000). The shift in the peak positions, bandwidths and intensities of the bands all give valuable structural and functional information, which may have diagnostic value (Liu et al. 1996; Yano et al. 1996; Ci et al. 1999; Severcan et al. 2000). The FTIR spectroscopy technique has been previously applied to investigate the effect of estradiol and tamoxifen on rat brain membranes (Dicko et al. 1999). It has also been established that FTIR spectroscopy has an increasingly important role to play in the field of pathology. Disease-induced changes can easily be detected with this technique. It has been used in the characterization of tissues from cancer, Alzheimer's disease, arthritis and multiple sclerosis (Gentner et al. 1998).

Materials and methods

After approval by the Ethics Committee, male Winstar albino rats were selected for our study with weights ranging between 250–320 g. They were divided into two groups: group 1 (five rats) was a control group without any treatment; group 2 (seven rats) was a chronically hypoperfused group.

In group 2, cephalic internal carotid artery to caudal external jugular vein anastomosis was performed as described by Spetzler et al. (1978) to bypass blood through the circle of Willis without perfusing the main brain vessels. Stealing of blood through the fistula resulted in chronic hypoperfusion of the brains over an eight-week waiting period, as reported by others (Morgan et al. 1989; Bederson et al. 1991). In group 2, chronic hypoperfusion resulted in hypoxia, proven by pathology revealing hippocampal neuronal cell loss and gliosis. Then, the rats were decapitated. Rat brain tissues were removed for FTIR spectroscopy analysis and stored at −80 °C.

Details of the surgery

Under general anesthesia of intraperitoneal ketamin/xylazin (90/10 mg/kg), and with the aid of an operation microscope and microsurgical techniques and instruments, the right common carotid artery, the right internal and external carotid arteries, the right common jugular vein and the right external jugular vein were identified and dissected. The right external carotid artery was ligated from its origin from the common carotid artery. The right common carotid artery was ligated caudally and the external jugular vein was ligated cephally. The right common carotid artery superior to ligation and the external jugular vein inferior to the ligation were cut using a micro-technique. The free ends were end-to-end anastomosed to each with interrupted 10/0 nylon sutures. In each anastomosis, the function of the fistula was tested with proximal and distal closing tests and confirmed.

Operated rats were kept in normal diurnal rhythm without restriction of any diet or activity for 8 weeks. At the end of 8 weeks, euthanasia was applied to all groups at the same time to decrease variability of the results and all rats were decapitated.

FTIR analysis

The brain samples were homogenized with saline phosphate buffer, pH 7.4, and centrifuged at 125,000×*g* for 15 min. Membrane-rich parts (pellet) of these homogenates were used for FTIR studies. FTIR spectra of samples were recorded at 3100–1000 cm^{-1}. Sample suspensions of 15 μL were placed between water-insoluble CaF_2 windows with 12 μm sample thickness. IR spectra were obtained using a Bomem 157 FTIR spectrometer (Michelson Series, Bomem, Quebec, Canada) equipped with a deuterated triglycine sulfate (DTGS) detector. The instrument was under continuous dry air purge to eliminate atmospheric water vapor. Interferograms were averaged for 400 scans at 4 cm^{-1} resolution.

Win Bomem Easy software (Galactic Industries Corporation) was used for the frequency measurements. The spectra of brain homogenates were subtracted from the spectrum of the buffer and the wavenumber values of all functional groups were recorded. The band positions were measured according to the center of weight. The spectra were normalized in specific regions for data analysis by using the same software. After the normalization process, the band areas were calculated using GRAMS/32 (Galactic Industries, Salem, NH, USA). An integration function was applied in the 2994–2949 cm^{-1} region for the area of the CH_3 asymmetric stretching band, in the 2866.5–2794 cm^{-1} region for the area of the CH_2 symmetric stretching band, in the 1709–1583 cm^{-1} region for the area of the amide I band, and in the 1583–1484 cm^{-1} region for the area of the amide II band. To find out the number of peaks in the amide I region for the curve fitting process, the second derivative spectra were calculated by using Win Bomem Easy software (Savitsky–Golay as derivative operation, nine points of smoothing) in the amide I region (1710–1585 cm^{-1}). After baseline correction, the best fit for decomposing the amide I bands in the region between 1710 cm^{-1} and 1585 cm^{-1} was obtained by Gaussian components using GRAMS/32. Band shape was considered Gaussian in all instances and the baseline was always linear. The band position and width of the first peak, corresponding to β-sheet antiparallel structure, was fixed at 1693 cm^{-1} (width 11 cm^{-1}); the sixth peak, corresponding to β-sheet structure, was fixed at 1633 cm^{-1} (width 40 cm^{-1}), but the other bands (at 1680 cm^{-1}, 1660 cm^{-1}, 1647 cm^{-1}, 1637 cm^{-1}) were left free. The process was iterated until a satisfactory fit between the computed and experimental band was obtained. The percentage areas of the sub-bands in the amide I region were calculated from the final fitted band areas. The fit was converged with a correlation (R^2) of 0.99–1 and a standard error of 0.001. Averages of the spectra belonging to the same experimental group were calculated by using GRAMS/32.

Statistics

The results were expressed as mean ± standard deviation. The differences in the means of the treated and control samples were compared using the Mann–Whitney U test. A P value of less than 0.05 was considered statistically significant ($P < 0.05$*, $P < 0.01$**, $P < 0.001$***).

Results and discussion

We have carried out FTIR spectroscopic studies on tissue homogenates from rat brain subjected to steal phenomena. The aim is to identify the biochemical and biophysical changes occurring in brain tissues as a result of hypoperfusion.

Table 1 shows changes in the band areas of the main functional groups in the 3000–1480 cm^{-1} region. As seen from the table, there are significant differences between hypoperfused brain and control brain samples, which will be discussed in detail.

Table 1 Changes in the band areas and area ratios of various functional groups in control ($n=5$) and hypoperfused ($n=7$) rat brain tissues (values are shown as mean ± standard deviation)

Functional groups	Control	Hypoperfused	*P* values
CH_3 asymmetric stretching	2.126 ± 0.009	1.776 ± 0.019	< 0.009**
CH_2 symmetric stretching	6.520 ± 0.010	6.600 ± 0.009	< 0.010**
Amide I	194.550 ± 0.100	178.586 ± 0.100	< 0.010**
Amide II	30.026 ± 0.070	27.419 ± 0.080	< 0.010**
AmideI/CH_2 symmetric stretching	29.830 ± 0.100	27.058 ± 0.101	< 0.008**

Figure 1 shows the average spectra in the 3000–2800 cm^{-1} region for both control and hypoperfused brain samples. Lipids are the major contributors in this spectral region (Mourant et al. 2003). Spectra were normalized with respect to the CH_2 asymmetric stretching band. The area of IR absorptions arising from a particular species is directly proportional to the concentration of that species. Thus, in principle, it is possible to determine the concentration of multiple analytes from a single spectrum, imparting a significant saving of time and labor (Jackson et al. 1997). The bands centered at 2956 cm^{-1} and 2923 cm^{-1} correspond to the stretching mode of asymmetrical CH_3 and CH_2 vibrations, respectively; the band centered at 2852 cm^{-1} corresponds to CH_2 symmetric stretching vibrations due to lipids (Melin et al. 2000). It is seen from Table 1 and Fig. 1 that there is a decrease in the area of the CH_3 asymmetric stretching mode in the hypoperfused brain tissues. This means that the number of methyl groups in the acyl chains of lipids in this group decreases (Takahashi et al. 1991). An increase in the area of the CH_2 symmetric stretching mode occurs with the application of operations on the rat brain, indicating an increase in phospholipids or fatty acid concentrations. This change in the lipid content might be important, because the cell lipids play several significant roles in the regulation of membrane function (Evans and Hardison 1985).

FTIR spectroscopy is one of the major techniques for the determination of protein secondary structures (Arrondo et al. 1993; Haris and Severcan 1999; Severcan and Haris 2003). Thus, FTIR spectroscopy offers unique possibilities for the simultaneous study of proteins together with lipid structures in biological membranes and tissues (Szalontai et al. 2000; Çakmak et al. 2003). Figure 2 shows the average spectra for both control and hypoperfused groups in the 1720–1480 cm^{-1} region. The spectra were normalized with respect to the CH_2 asymmetric stretching band. The bands around 1647 cm^{-1} and 1549 cm^{-1} are attributable to amide I and amide II vibrations of structural proteins, respectively (Manoharan et al. 1993; Haris and Severcan 1999). It is clearly seen in Table 1 that the areas of the amide I and amide II bands decrease in the hypoperfused group. This decrease in the content of protein can be due to the disruption of protein synthesis which occurs in the case of decreased cerebral blood flow and consequently ATP depletion in hypoperfused brain samples (Fieschi et al. 1990; Wang et al. 2000). In addition to this, it wasreported previously that amino acid formation is reduced after ischemic insult, which may also explain the observed decrease in the protein content in the hypoperfused brain samples in our case (Sutherland et al. 1990).

An important factor affecting the membrane structure and dynamics is the amount of proteins and lipids in the membranes (Szalontai et al. 2000). From the FTIR spectrum, a precise protein-to-lipid ratio can be derived by calculating the ratio of the areas of the bands arising from lipids and proteins. As it is seen in Table 1, the ratio of the area of the amide I band to the area of the CH_2 symmetric stretching absorptions decreases in the hypoperfused group. Generally, this decrease in the ratio suggests a decrease in the protein content or an

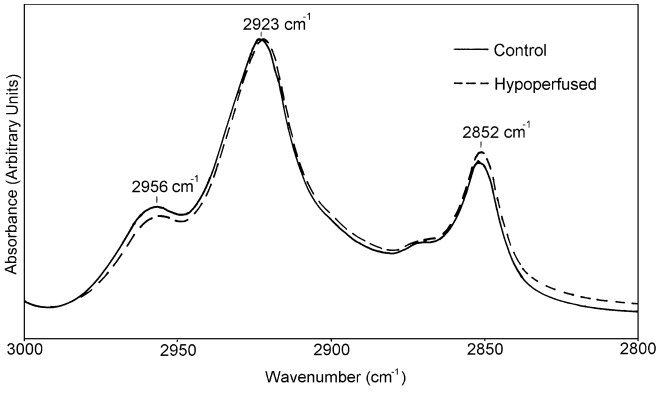

Fig. 1 The average spectra of control ($n=5$) and hypoperfused ($n=7$) brain samples in the 3000–2800 cm^{-1} region. The spectra were normalized with respect to the CH_2 asymmetric stretching band

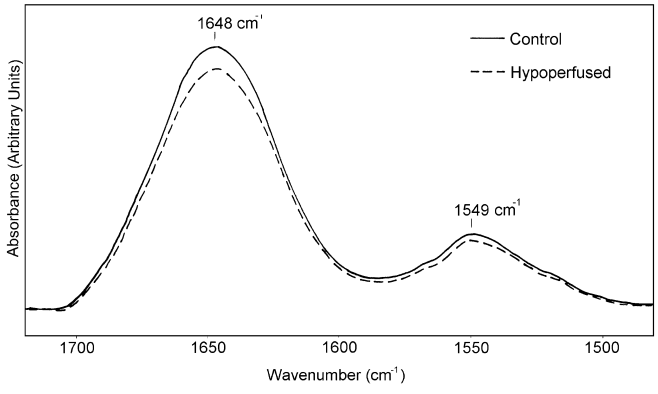

Fig. 2 The average spectra of control ($n=5$) and hypoperfused ($n=7$) brain samples in the 1720–1480 cm^{-1} region. The spectra were normalized with respect to the CH_2 asymmetric stretching band

Table 2 Changes in the frequency (wavenumber) values of various functional groups in control ($n = 5$) and hypoperfused ($n = 7$) rat brain tissues (values are shown as mean ± standard deviation)

Functional groups	Control	Hypoperfused	*P* values
CH_3 asymmetric stretching	2956.60 ± 0.13	2955.50 ± 0.13	< 0.008**
CH_2 asymmetric stretching	2922.90 ± 0.12	2922.20 ± 0.10	< 0.008**
CH_2 symmetric stretching	2851.80 ± 0.13	2851.40 ± 0.09	< 0.008**

increase in the lipid content, or both (Jackson et al. 1997). In our case, the increase in the lipid content in the hypoperfused groups is supported by the significant increase in the area of the CH_2 symmetric stretching vibrations, whilst the decrease in the protein content is supported by the decrease in the areas of both the amide I and amide II bands. All these results support the finding that the lipid-to-protein ratio increases in the hypoperfused brain samples.

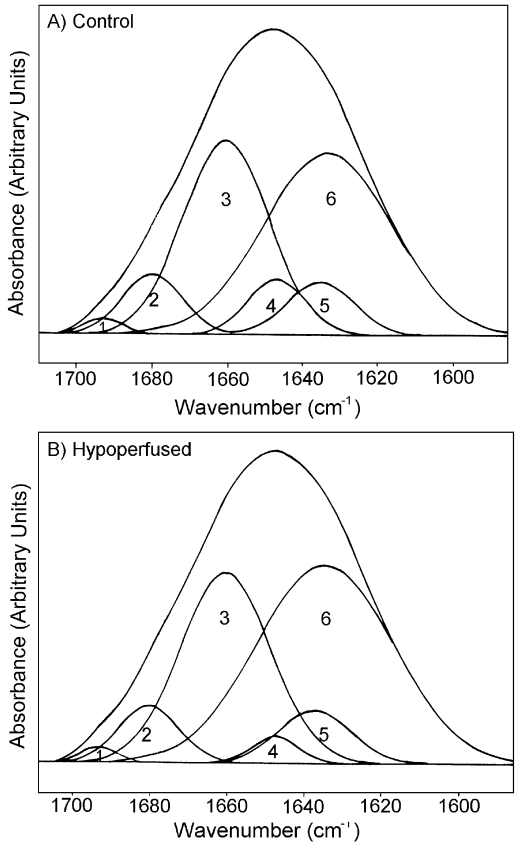

Fig. 3 **A** The underlying amide I bands in the 1710–1585 cm^{-1} region, as deduced by curve-fitting analysis for average spectra of the control ($n = 5$); **B** the average spectra of the hypoperfused ($n = 7$) brain samples. Peak 1 refers to β-sheet antiparallel structure; peak 2 refers to β-turn structure; peak 3 refers to unordered α-helix structure; peak 4 refers to α-helix structure; peak 5 refers to random coil structure; peak 6 refers to β-sheet structure

The frequency of the absorptions provides information relating to structure/conformation and intermolecular interactions (Jackson et al. 1997, 1999; Toyran et al. 2003). The changes in the wavenumber (frequency) values are given in Table 2. The table shows that there is a significant decrease in the frequency of the CH_2 symmetric and asymmetric vibrations upon the induction of hypoperfusion in the rat brain. This indicates an increase in the state-of-order in lipids (Kneipp et al. 2000).

The changes in the deep interior of the bilayer were monitored by the wavenumber of the CH_3 asymmetric stretching mode. An increase in the frequency of this band reflects increasing librational freedom of the acyl chains in the central area of the bilayer, and a decrease in the frequency corresponds to stiffness of the bilayer (Umemura et al. 1980). As is seen in Table 2, there is a decrease in the frequency of the CH_3 asymmetric stretching mode, revealing that application of the operation decreases the librational freedom of the acyl chains of the phospholipids in the central area of the bilayer of rat brain homogenates.

The amide I region, around 1646 cm^{-1} in our case, is useful for the determination of protein secondary structure (Lyman and Murray-Wijelath 1999). We have carried out further analysis of proteins present in the brain samples by resolving the amide I band using band-fitting methods to have a better understanding of the effect of hypoperfusion on protein structure at the molecular level. In the amide I region (1710–1585 cm^{-1}), the underlying bands contributing to the baseline-corrected spectra were determined using a combination of second-derivative and curve-fitting functions. Firstly, by using a second-derivative arithmetical function, six peaks and their relative positions were determined. In Fig. 3 the peak around 1693 cm^{-1}, labelled as 1, arises from β-sheet antiparallel structure; the peak around 1680 cm^{-1}, labelled as 2, arises from β-turn structure;

Table 3 Summary of results of the curve-fitting analysis expressed as a function of percentage areas of main protein secondary structures for control ($n = 5$) and hypoperfused ($n = 7$) rat brain samples (values are shown as mean ± standard deviation)

Structure	Peak centers (cm^{-1})	Area (%) Control	Area (%) Hypoperfused	*P* values
α-Helix	1660, 1647	39.05 ± 1.73	35.95 ± 1.18	< 0.05*
β-Sheet	1693, 1680, 1633	53.33 ± 1.02	56.06 ± 1.60	< 0.05*
Random coil	1637	7.03 ± 0.92	8.06 ± 0.66	< 0.14

the peak around 1660 cm^{-1}, labelled as 3, is due to unordered α-helix structure; the peak around 1647 cm^{-1}, labelled as 4, arises from α-helix structure; the peak around 1637 cm^{-1}, labelled as 5, is assigned to random coil structure; and the peak around 1633 cm^{-1}, labelled as 6, is assigned to β-sheet structure (Cadrin et al. 1991; Takahashi et al. 1991; Kochan et al. 1995; Hendler et al 2003). The second derivative of the original spectra offers a direct way to identify the peak frequencies of the characteristic components and thus permits much more detailed qualitative study (Susi and Byler 1983).

The underlying amide I bands as deduced by curve-fitting analysis for control and hypoperfused groups are given in Fig. 3. The best fit for decomposing the complex feature of the amide I band was obtained by Gaussian curves. The percentage areas of the main protein secondary structures obtained after curve-fitting analysis are given in Table 3 for both control and hypoperfused brain samples. It can be deduced from these results that hypoperfusion causes a significant decrease in the content of α-helical structures and a significant increase in the content of β-sheet structures. These results, together with a slight increase in the content of random coil structures, imply that denaturation of the proteins might be taking place. Another possibility for the increase in the β-sheet structures is that there may be an overexpression of β-amyloid precursor protein in the hypoperfused brain, which was the case in a previous study on rodent models (Shi et al. 2000). Furthermore, the changes we have observed in the secondary structure of proteins in hypoperfused tissues were indirectly supported by previous studies with other techniques, such as Western blotting (Kurumatani et al. 1998), SDS gel electrophoresis and immunoblot methods (Ogata 1989). In our study, by considering the increase in the β-sheet and random coil structures, we can deduce that proteins might be seriously affected in the hypoperfused brain. One possible explanation for this effect may be intracellular acidosis, which occurs as a result of the combined extrusion of H^+ ions and lactate accumulation during ischemia/hypoxia (Siesjo 1988; Plaschke et al. 2000; Schurr 2002). The increase in anaerobic glycolysis, in which glucose is converted to lactate, and the decrease in lactate clearance under hypoperfused conditions, leads to lactate accumulation (Fieschi et al. 1990; Ueda et al. 2000). Lowering the pH can cause some changes in the protein structure and function, which may result in gross membrane dysfunction (Siesjo 1988).

In conclusion, the results of this work suggest that hypoperfusion causes significant effects on the structure and content of lipids and proteins in rat brain homogenates. An increase in the lipid content, a decrease in the protein content and an increase in the lipid-to-protein ratio were observed. The state of order of lipids increases in the hypoperfused rat brain samples. FTIR results also revealed that the proteins are affected in terms of content and secondary structure in favor of β-sheets and random coils.

Acknowledgements This work was supported by The Scientific and Technical Research Council of Turkey, SBAG-2320 research fund, and TÜBİTAK-BAYG (The Scientific and Technical Research Council of Turkey – Directorate of Human Resources Development).

References

Alici K, Heinemann U (1995) Effects of low glucose levels on changes in $[Ca^{2+}]_o$ induced by stimulation of Schaffer collaterals under conditions of blocked chemical synaptic transmission in rat hippocampal slices. Neurosci Lett 185:5–8

Alici K, Weber-Luxenburger G, Heinemann U (1998) Effects of glucose deprivation in area CA1 of hippocampal slices from adult and juvenile rats. Brain Res Dev Brain Res 107:71–80

Arrondo JL, Muga A, Castresana J, Goni FM (1993) Quantitative studies of the structure of proteins in solution by Fourier-transform infrared spectroscopy. Prog Biophys Mol Biol 59:23–56

Bederson JB, Wiestler OD, Brusstle O, Roth P, Frick R, Yasargil MG (1991) Intracranial venous hypertension and the effects of venous out flow obstruction in a rat model of arterio-venous fistula. Neurosurgery 29:341–351

Cadrin M, French SW, Wong PT (1991) Alteration in molecular structure of cytoskeleton proteins in griseofulvin-treated mouse liver: a pressure tuning infrared spectroscopy study. Exp Mol Pathol 55:170–179

Çakmak G, Togan I, Uğuz C, Severcan F (2003) FT-IR spectroscopic analysis of rainbow trout liver exposed to nonylphenol. Appl Spectrosc 57:835–841

Choo LP, Jackson M, Halliday WC, Mantsch HH (1993) Infrared spectroscopic characterisation of multiple sclerosis plaques in the human central nervous system. Biochim Biophys Acta 1182:333–337

Ci YX, Gao TY, Feng J, Guo ZQ (1999) FTIR spectroscopic characterization of human breast tissue: implications for breast cancer diagnosis. Appl Spectrosc 53:312–315

de Wilde MC, Farkas E, Gerrits M, Kiliaan AJ, Luiten PG (2002) The effect of *n*−3 polyunsaturated fatty acid-rich diets on cognitive and cerebrovascular parameters in chronic cerebral hypoperfusion. Brain Res 947:166–173

Dicko A, Morissette M, Ben Ameur S, Pezolet M, Di Paolo T (1999) Effect of estradiol and tamoxifen on brain membranes: investigation by infrared and fluorescence spectroscopy. Brain Res Bull 49:401–405

Diem M, Boydston-White S, Chiriboga L (1999) Infrared spectroscopy of cells and tissues: shining light onto a novel subject. Appl Spectrosc 53:148A–161A

Evans WH, Hardison WG (1985) Phospholipid, cholesterol, polypeptide and glycoprotein composition of hepatic endosome subfractions. Biochem J 15:33–36

Fabian H, Jackson M, Murphy L, Watson PH, Fichtner I, Mantsch HH (1995) A comparative infrared spectroscopic study of human breast tumors and breast tumor cell xenografts. Biospectroscopy 1:37–46

Fieschi C, Di Piero V, Lenzi GL, Pantano P, Giubilei F, Puttinelli C, Carolei A (1990) Pathophysiology of ischemic brain disease. Stroke (Suppl IV) 21:IV9–IV11

Fleidervish IA, Gebhardt C, Astman N, Gutnick MJ, Heinemann U (2001) Enhanced spontaneous transmitter release is the earliest consequence of neocortical hypoxia that can explain the disruption of normal circuit function. J Neurosci 21:4600–4608

Gentner JM, Wentrup-Byrene E, Walker PJ, Walsh MD (1998) Comparison of fresh and post-mortem human arterial tissue: an analysis using FT-IR microspectroscopy and chemometrics. Cell Mol Biol 44:251–259

Haris PI, Severcan F (1999) FTIR spectroscopic characterization of protein structure in aqueous and non-aqueous media. J Mol Catal B 7:207–221

Hendler RW, Barnett SM, Dracheva S, Bose S, Levin IW (2003) Purple membrane lipid control of bacteriorhodopsin conformational flexibility and photocycle activity. Eur J Biochem 270:1920–1925

Hofmeister C, Stapf C, Hartmann A, Sciacca RR, Mansmann U, terBrugge K, Lasjaunias P, Mohr JP, Mast H, Meisel J (2000) Demographic, morphological, and clinical characteristics of 1289 patients with brain arteriovenous malformation. Stroke 31:1307–1310

Jackson M, Sowa MG, Mantsch HH (1997) Infrared spectroscopy: a new frontier in medicine. Biophys Chem 68:109–125

Jackson M, Mansfield JR, Dolenko B, Somorjai RL, Mantsch HH, Watson PH (1999) Classification of breast tumors by grade and steroid receptor status using pattern recognition analysis of infrared spectra. Cancer Detect Prev 23:245–253

Kawaguchi C, Takizawa S, Niwa K, Iwamoto T, Kuwahira I, Kato H, Shinohara Y (2002) Regional vulnerability to chronic hypoxia and chronic hypoperfusion in the rat brain. Pathophysiology 8:249–253

Kneipp J, Lasch P, Baldauf E, Beekes M, Naumann D (2000) Detection of pathological alterations in scrapie-infected hamster brain by FTIR spectroscopy. Biochim Biophys Acta 1501:189–199

Kochan Z, Karbowska J, Bukato G, Zydowo MM, Bertoli E, Tanfani F, Swierczynski J (1995) A comparison of the secondary structure of human brain mitochondrial and cytosolic 'malic' enzyme investigated by Fourier-transform infrared spectroscopy. Biochem J 309:607–611

Kral T, Luhmann HJ, Mittmann T, Heinemann U (1993) Role of NMDA receptors and voltage-activated calcium channels in an in vitro model of cerebral ischemia. Brain Res 612:278–288

Kurumatani T, Kudo T, Ikura Y, Takeda M (1998) White matter changes in the gerbil brain under chronic cerebral hypoperfusion. Stroke 29:1058–1062

Liu K, Jackson M, Sowa MG, Ju H, Dixon IMC, Mantsch HH (1996) Modification of the extracellular matrix following myocardial infarction monitored by FTIR spectroscopy. Biochim Biophys Acta 1315:73–77

Liu K, Bose R, Mantsch HH (2002) Infrared spectroscopic study of diabetic platelets. Vibrat Spectrosc 28:131–136

Lyman DJ, Murray-Wijelath J (1999) Vascular graft healing: FTIR analysis of an implant model for studying the healing of a vascular graft. J Biomed Mater Res 48:172–186

Manoharan R, Baraga JJ, Rava RP, Dasari RR, Fitzmaurice M, Feld MS (1993) Biochemical analysis and mapping of atherosclerotic human artery using FT-IR microspectroscopy. Atherosclerosis 103:181–193

Melin A, Perromat A, Deleris G (2000) Pharmacologic application of Fourier transform IR spectroscopy: in vivo toxicity of carbon tetrachloride on rat liver. Biopolymers (Biospectroscopy) 57:160–168

Morgan MK, Anderson RE, Sundt TM (1989) The effect of hyperventilation on cerebral blood flow in the rat with open and closed carotid-jugular fistula. Neurosurgery 25:606–612

Mourant JR, Yamada YR, Carpenter S, Dominique LR, Freyer JP (2003) FTIR spectroscopy demonstrates biochemical differences in mammalian cell cultures at different growth stages. Biophys J 85:1938–1947

Ogata N (1989) Degradation of cytoskeletal proteins in cerebral ischemia. Nippon Geka Hokan 58:71–79

Plaschke K, Weigand MA, Michel A, Martin E, Bardenheuer HJ (2000) Permanent cerebral hypoperfusion: 'preconditioning-like' effects on rat energy metabolism towards acute systemic hypotension. Brain Res 858:363–370

Roman GC, Erkinjuntti T, Wallin A, Pantoni L, Chui CH (2002) Subcortical ischemic vascular dementia. Lancet Neurol 1:426–436

Schurr A (2002) Energy metabolism, stress hormones and neural recovery from cerebral ischemia/hypoxia. Neurochem Int 41:1–8

Severcan F, Haris PI (2003) Fourier transform infrared spectroscopy suggests unfolding of loop structures precedes complete unfolding of pig citrate synthase. Biopolymers 69:440–447

Severcan F, Toyran N, Kaptan N, Turan B (2000) Fourier transform infrared study of the effect of diabetes on rat liver and heart tissues in the C–H region. Talanta 53:55–59

Shi J, Yang SH, Stubley L, Day AL, Simpkins JW (2000) Hypoperfusion induces over expression of β-amyloid precursor protein mRNA in a focal ischemic rodent model. Brain Res 853:1–4

Siesjo BK (1988) Mechanisms of ischemic brain damage. Crit Care Med 16:954–963

Sills RH, Moore DJ, Mendelsohn R (1994) Erythrocyte peroxidation: quantitation by Fourier transform infrared spectroscopy. Anal Biochem 218:118–123

Spetzler RF, Wilson CB, Weistein P, Mehdorn M, Townsend J, Telles D (1978) Normal perfusion pressure breakthrough theory. Clin Neurosurg 25:651–672

Susi H, Byler DM (1983) Protein structure by Fourier transform infrared spectroscopy: second derivative spectra. Biochem Biophys Res Commun 115:391–397

Sutherland G, Peeling J, Lesiuk H, Saunders J (1990) Experimental cerebral ischemia studied using nuclear magnetic resonance imaging and spectroscopy. Can Assoc Radiol J 41:24–31

Szalontai B, Nishiyama Y, Gombos Z, Murata N (2000) Membrane dynamics as seen by Fourier transform infrared spectroscopy in a cyanobacterium, *Synechocystis* PCC 6803. The effects of lipid unsaturation and the protein-to-lipid ratio. Biochim Biophys Acta 1509:409–419

Takagi Y, Hattori I, Nozaki K, Ishikawa M, Hashimoto N (2000) DNA fragmentation in central nervous system vascular malformations. Acta Neurochir (Wien) 142:987–994

Takahashi H, French SM, Wong PTT (1991) Alteration in hepatic lipids and proteins by chronic ethanol intake: a high pressure Fourier transform infrared spectroscopic study on alcoholic liver disease in the rat. Alcoholism Clin Exp Res 15:219–223

Toyran N, Severcan F (2003) Competitive effect of vitamin D_2 and Ca^{2+} on phospholipid model membranes: an FTIR study. Chem Phys Lipids 123:165–176

Ueda M, Muramatsu H, Kamiya T, Muramatsu A, Mori T. Terashi A, Katayama Y (2000) Pyruvate dehydrogenase activity and energy metabolite levels following bilateral common carotid artery occlusion in rat brain. Life Sci 67:821–826

Umemura J, Cameron DG, Mantsch HH (1980) A Fourier transform infrared spectroscopic study of the molecular interaction of cholesterol with 1,2-dipalmitoyl-*sn*-glycero-3-phosphocholine. Biochim Biophys Acta 602:32–44

Wang LM, Han YF, Tang XC (2000) Huperzine A improves cognitive deficits caused by chronic cerebral hypoperfusion in rats. Eur J Pharmacol 398:65–72

Wetzel DL, Slatkin DN, Levine SM (1998) FT-IR microspectroscopic detection of metabolically deuterated compounds in the rat cerebellum: a novel approach for the study of brain metabolism. Cell Mol Biol (Noisy-le-Grand) 44:15–27

Yamada K, Ji JJ, Yuan H, Miki T, Sato S, Horimoto N, Shimizu T, Seino S, Inagaki N (2001) Protective role of ATP-sensitive potassium channels in hypoxia-induced generalized seizure. Science 292:1543–1546

Yano K, Ohoshima S, Shimizu Y, Moriguchi T, Katayama H (1996) Evaluation of glycogen level in human lung carcinoma tissues by an infrared spectroscopic method. Cancer Lett 110:29–34